Dynamic Simulation and Nonlinear-Model-Based Product Quality Control of a Crude Tower

Chang-Bock Chung
Dept. of Fine Chemical Engineering, Chonnam National University, Kwangju 500-757, Korea

James B. Riggs
Dept. of Chemical Engineering, Texas Tech University, Lubbock, TX 79409

The dynamic stagewise adiabatic flash algorithm is applied to the dynamic simulation of a crude column. This algorithm is based on the implicit integration of the model equations of each stage and the explicit combination of the stage models to form the column model. Stable, efficient integration for the crude column model is observed with simulation CPU requirements that are 20 times faster than real time using a 50 MHz 486 P.C. Specific dynamics of a crude column are identified such as one-way interaction and inverse action. The dynamic crude column model is used to study product quality control of a crude column using nonlinear-process-model-based control (PMBC) which was tested using two different steady-state controller models for setpoint tracking and disturbance rejection. Both nonlinear PMBC controllers show good control performance, but are limited by the inherent inverse action of the crude column. Control results for a set of single-loop PI controllers is also presented as a point of reference.

Introduction

A crude tower is the first processing unit in a refinery and separates crude, which is a continuum of components ranging from methane to asphalt, into several boiling-range fractions. These fractions become either products or feedstocks for downstream processing units. The crude unit is a highly energy-consuming process, and usually has complicated flow and heat integration structures. Since any upset in the tower will propagate to downstream processing units, it is of utmost importance to maintain the crude tower product quality on specification.

The product quality control of a crude tower usually constitutes a highly interacting multivariable system. Due to its complexity, most publications on crude unit control have been concerned with computer control schemes (Adams, 1962; Van Horn and Latour, 1976; Wade et al., 1977; Friedman, 1985; Veland et al., 1987; Muske et al., 1991a,b). In these publications, most of the authors have described their experiences with advanced control projects for commercial units. Linear-model-based predictive control [such as dynamic matrix control (DMC)] (Cutler and Ramaker, 1979) and IDCOM (Richalet et al., 1978) appear to represent the major control algorithm implemented in recent commissioning activities for crude units. Benefits from these projects were reported to include improved product qualities, yields, and energy saving.

The objective of this work is to investigate nonlinear-process-model-based control (PMBC) for crude tower product quality control using a simulated crude tower. A major emphasis was placed on the understanding of the dynamic behavior of a crude tower in open-loop and closed-loop modes. This was achieved by the development of a new dynamic simulation algorithm.

Nonlinear PMBC refers to methods that use a nonlinear approximate process model directly for control purposes, without linearization. Several types of nonlinear PMBC methods have been developed in recent years including generic model control (GMC) (Lee and Sullivan, 1988), nonlinear internal model control (NLIMC) (Economou et al., 1986), and nonlinear predictive model control (NLPMC) (Parrish and Brosilow, 1988). The review article by Bequette (1991) provides an overview of the nonlinear PMBC field. In this work a GMC structure using a steady-state approximate model of the process was used for crude tower product quality control.

A diagram of the model crude tower used in this work is

Correspondence concerning this article should be addressed to J. B. Riggs.

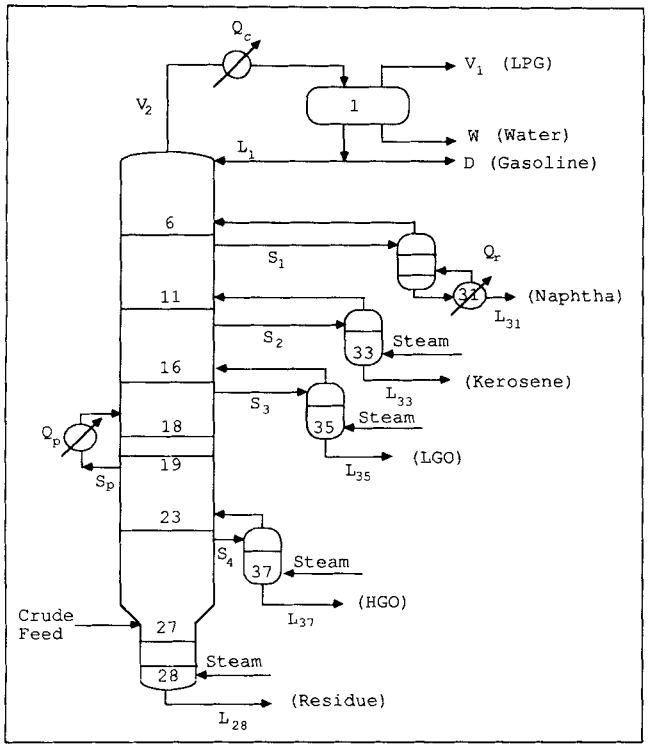

Figure 1. Theoretical analogue of an Exxon crude tower.

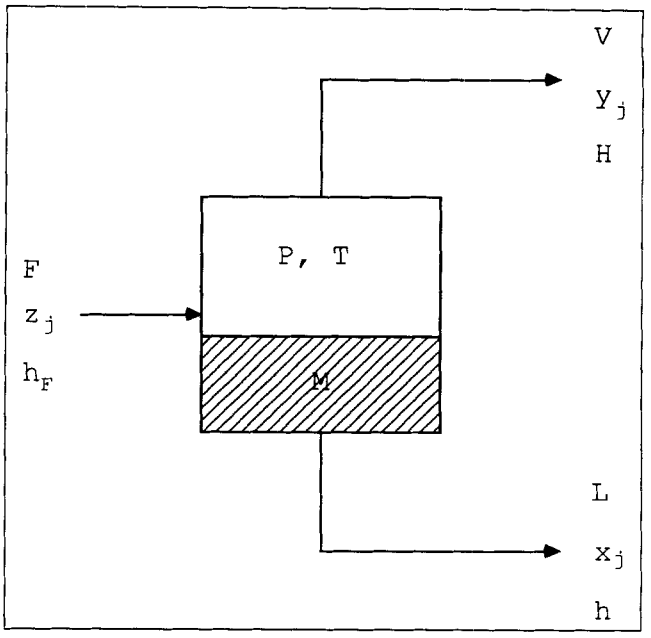

Figure 2. Single flash stage.

shown in Figure 1. The tower is a theoretical analogue of a 62-stage Exxon crude tower originally studied by Cecchetti et al. (1963), who applied the θ-method of convergence for obtaining a steady-state solution that matched the field data. The tower was also used in several studies using the 2N Newton-Raphson method for a steady-state solution (Hess et al., 1977; Holland, 1981), and for dynamic simulation and control using a quadratic dynamic matrix control algorithm (Hsie, 1989). In all the studies, the crude feed was divided into 35 pseudo-components (including added water) in order to represent the true-boiling-point curve. The physical properties of the pseudo-components originally presented by Cecchetti et al. (1963) were curve fitted by Hess (1977) to correlate the equilibrium K values and enthalpies as functions of temperature only. This approach was also used in this work.

In this article the dynamic simulation of a single flash stage is discussed, followed by single-stage models combined to form a model for an entire crude tower and open-loop responses are discussed in relation to the product quality control of the tower. Finally, nonlinear PMBC schemes employing two kinds of steady-state models are presented, and their control performances are evaluated for setpoint tracking and feed disturbance rejection.

Dynamic Simulation of Single Flash Stage

Dynamic model

Figure 2 shows a single flash stage where a feed stream splits into vapor and liquid streams. Assuming an equilibrium stage and a negligible vapor holdup, a dynamic model for the flash stage can be easily derived as follows:

(Holdup)

$$\frac{dM}{dt} = F - L - V \tag{1}$$

(Composition)

$$\frac{dx_j}{dt} = \frac{F(z_j - x_j) - V(y_j - x_j)}{M}, \quad j = 1, \ldots, C \tag{2}$$

(Enthalpy)

$$\frac{dh}{dt} = \frac{F(h_F - h) - V(H - h)}{M} \tag{3}$$

(Equilibrium)

$$y_j = K_j(T)x_j, \quad j = 1, \ldots, C \tag{4}$$

(Summation)

$$\sum_{j=1}^{C} x_j = 1 \tag{5}$$

$$\sum_{j=1}^{C} y_j = 1 \tag{6}$$

(Weir)

$$M = f_w(L) \tag{7}$$

Specification of the feed condition and the stage pressure is

enough to define the stage completely, and the problem thus reduces to a *dynamic adiabatic flash calculation*. A typical solution procedure consists of numerical time integration from given initial values of the dependent variables of Eqs. 1-3. The differential equations, however, involve two variables, V and T, which are not known explicitly yet and have to be found before time integration starts.

Bubble point algorithm and its instability

The most popular distillation algorithm has been the bubble point (BP) algorithm whereby V is calculated from the energy balance (Eq. 3) and T from a bubble point calculation (Friday and Smith, 1964). For a steady-state solution, the BP algorithm usually involves a double-loop iterative search for V and T. For a dynamic solution, strictly speaking, the dual iteration should be repeated at each time step. To avoid excessive computation time, however, it is customary to bypass the iteration for V by determining it from a transformed algebraic energy balance equation (Gani et al., 1986). Once V is found for use during the current step, the composition and temperature can be solved using either explicit or implicit integration rules. The choice of a numerical integration scheme largely depends on the stiffness of the system.

Transformation of a differential energy balance equation into an algebraic one may take several forms. The simplest and most popular scheme is to assume constant molar enthalpy ($dh/dt = 0$) (Frank, 1972) during a small time step. A correction for this assumption would be to approximate the derivative by taking finite differences between two successive steps. Ballad and Brosilow (1978) derived complicated algebraic equations by expanding an enthalpy derivative in terms of composition derivatives on the basis of thermodynamic relationships, followed by substitution of the righthand-side terms of the composition equations. This approach was adopted by Hsie (1989) for the dynamic simulation of the Exxon crude tower.

A BP algorithm was used to solve the dynamic model of a single flash stage formed by the flashing of the Exxon crude feed. But under a constant enthalpy assumption the algorithm failed to provide a stable solution. Figure 3 illustrates the breakdown of the algorithm when a 5% step change in feed enthalpy which was introduced to the initial steady state of the stage at time equal to zero. The instability could not be overcome by using smaller time steps or implicit integration schemes for the BP algorithm even for extremely small changes in inlet feed condition.

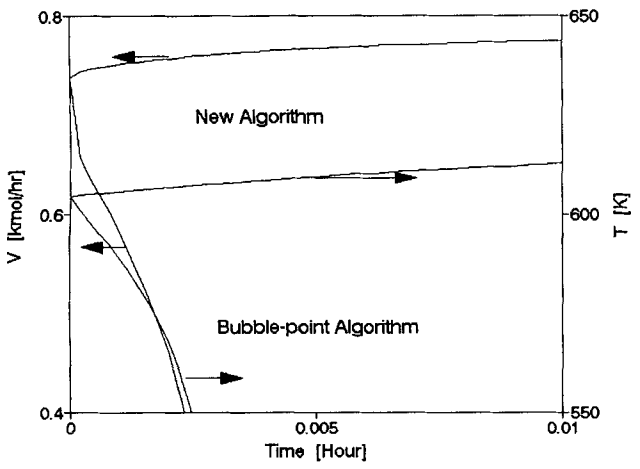

Figure 3. Single flash stage responses to 5% step increase in h_F.

The instability of the BP algorithm was found to originate from the *enthalpy inversion* of the system in the sense that its molar liquid enthalpy h is larger than molar vapor enthalpy H. Although, of course, each pure component liquid enthalpy, h_j, is always smaller than the pure component vapor enthalpy, H_j, still the mole-fraction-averaged mixture enthalpies can be inverted when $x_j \gg y_j$ for the heavy components. This situation may take place in the flashing of extremely wide-boiling feed mixture like crude where most heavy components would reside in the liquid phase rather than vaporize. Under this enthalpy inversion, the initial vapor flow rate calculated from Eq. 3 assuming $dh/dt = 0$ became smaller than its base level in the face of an increase in feed enthalpy. It is not difficult to show that this reduced vapor rate, which is contrary to our physical intuition, is just an initiation of a vicious cycle leading to the breakdown shown in Figure 3. It is noteworthy that the enthalpy inversion was encountered in 17 trays that constitute approximately the bottom half of our model crude tower shown in Figure 1 at the base case operating conditions.

Instability of the BP algorithm is not limited to the case of constant enthalpy assumed in calculating a vapor flow rate. In fact, approximation of the enthalpy derivative using finite differences increased the rate of breakdown because V became even smaller at each time step. Hsie (1989) also reported difficulties in obtaining a stable transient solution for the crude tower with enthalpy derivatives transformed based on thermodynamic relations.

Implicit Single Stage Model (ISS Model)

The instability of the BP algorithm arises from an unsuccessful attempt to calculate V only using an energy balance. In our approach, we find V and T simultaneously which will satisfy the mass and energy balances together. Given the condition at time step $t^{(n)}$, the algorithm proceeds in three steps as follows.

Step 1. Advance the time step to $t^{(n+1)}$, and approximate the derivatives in Eqs. 1-3 using backward finite differences to get:

$$\frac{M^{(n+1)} - M^{(n)}}{\Delta t} = F^{(n+1)} - L^{(n+1)} - V^{(n+1)} \tag{8}$$

$$\frac{x_j^{(n+1)} - x_j^{(n)}}{\Delta t} = \frac{F^{(n+1)}(z_j^{(n+1)} - x_j^{(n+1)}) - V^{(n+1)}(y_j^{(n+1)} - x_j^{(n+1)})}{M^{(n+1)}}, \quad j = 1, \ldots, C \tag{9}$$

$$\frac{h^{(n+1)} - h^{(n)}}{\Delta t} = \frac{F^{(n+1)}(h_F^{(n+1)} - h^{(n+1)}) - V^{(n+1)}(H^{(n+1)} - h^{(n+1)})}{M^{(n+1)}} \tag{10}$$

Step 2. Set up a two-element independent vector θ and a function which measures the mismatches in mass and energy balances:

$$\theta = \begin{pmatrix} \theta_1 \\ \theta_2 \end{pmatrix} = \begin{pmatrix} V^{(n+1)} \\ T^{(n+1)} \end{pmatrix} \tag{11}$$

$$f = \begin{pmatrix} f_1 \\ f_2 \end{pmatrix} = \begin{pmatrix} \sum_{j=1}^{C} (y_j - x_j) \\ \dfrac{M^{(n+1)} \dfrac{h^{(n+1)} - h^{(n)}}{\Delta t} + F^{(n+1)} h^{(n+1)} + V^{(n+1)} (H^{(n+1)} - h^{(n+1)})}{F^{(n+1)} h_F^{(n+1)}} - 1 \end{pmatrix} \tag{12}$$

Step 3. Starting from an initial guess $\theta = (V^{(n)}, T^{(n)})^T$, find a solution of $f = 0$ using the Newton-Raphson method.

In step 2, V and T were called the independent variables since all the other (dependent) variables can be found (using Eqs. 4, 6, 7, 8, and 9) once V and T are specified as the Newton-Raphson vector θ is updated at each iteration.

Stable solutions were obtained using this algorithm. Figure 3 shows that both V and T steadily approach a new steady state for 5% step change in feed enthalpy. Numerical stability was not endangered by the atypical enthalpy behavior of the crude feed since the calculation of V was based on both mass and energy balances. An implicit integration scheme adopted in step 1 above permitted larger time steps for faster computation without degrading the stability or the accuracy of the solutions significantly.

The proposed algorithm can be regarded as a dynamic version of the 2N Newton-Raphson algorithm (Holland, 1981) for the special case of $N = 1$, where N is the number of stages in a column. A fast Newton-Raphson convergence was obtained because the unknown vector only consisted of two variables (V and T) and each liquid mole fraction x_j could be directly calculated from Eq. 9. This resulted from the assumed ideal thermodynamic behavior of the pseudo-components of the crude. For nonideal mixtures whose K values also depend on liquid and vapor compositions, an iterative scheme will be required to calculate the compositions, which would increase the computation time.

It is noteworthy to mention that the enthalpy inversion problem can be avoided using another approach based on a BP algorithm. When the energy balance is written in terms of the total energy holdup, $E (= Mh)$, the enthalpy (Eq. 3) is replaced by:

$$\frac{dE}{dt} = Fh_F - Lh - VH \tag{13}$$

Then assuming $dE/dt = 0$,

$$V = (Fh_F - Lh)/H \tag{14}$$

which would give an increased V for an increase in h_F, thus appear to eliminate the enthalpy inversion problem. In applying Eq. 14, L is first calculated from the holdup at the current time step using Eq. 7. There are circumstances, however, where L is not known beforehand and thus has to be found simultaneously with V. For example, consider the case where a "perfect" level control is in effect (that is, $L = F - V$ all the time to maintain M constant). Then, V will be again calculated:

$$V = F(h_F - h)/(H - h) \tag{15}$$

which would give V in the wrong direction under the enthalpy inversion. A similar situation will be encountered when one attempts to solve a steady-state model using the same approach.

In addition to the stability problem, there are still two problems with this approach:

(1) Since this formulation is explicit, the integration step size would be limited by the stiffness of the equations. Due to the wide boiling nature of crude, the stiffness of the problem is quite severe requiring exceedingly small integration step sizes. In addition, as operating conditions change, stable step size requirements are likely to change.

(2) The assumption that $dE/dt = 0$ is less accurate than assuming $dh/dt = 0$ since E contains both changes in M and h. Changes in M occur on a relatively short time basis due to liquid dynamics while changes in h are due to composition changes which occurs at a much slower rate. Therefore, assuming that dh/dt is equal to zero appears to be a much more accurate assumption. Note that Eq. 3 is derived starting with Eq. 13 using the chain rule of differentiation with Eq. 1.

Dynamic Simulation of a Crude Tower

Dynamic model

The dynamic model described here was used as the "crude column process" to study crude column quality control performance. A dynamic model for the crude tower shown in Figure 1 was developed under the following assumptions:

1) Perfectly mixed, equilibrium stages
2) Negligible vapor holdups
3) Constant pressures on trays
4) Two immiscible liquid phases (hydrocarbon and water) in the accumulator.

Since the crude tower has a complicated flow structure due to side draws and a pumparound, the following conventions were used for flow rates to handle a general flow situation around stage i as shown in Figure 4 where:

L_i = flow rate of liquid leaving stage i and entering stage $i+1$, kmol/h
L_{i-1} = flow rate of liquid entering stage $i = L_{i-1} + S_{Li}$, kmol/h
L_i = flow rate of liquid leaving stage $i = L_i + S_{Li}$, kmol/h
V_i = flow rate of vapor leaving stage i and entering stage $i-1$, kmol/h
V_{i+1} = flow rate of vapor entering stage $i = V_{i+1} + S_{Vi}$, kmol/h
V_i = flow rate of vapor leaving stage $i = V_i + S_{Vi}$, kmol/h

Model 2 for the behavior of the feed plate (Holland, 1981) was adopted whereby the preflashed vapor feed and liquid feed streams were treated as coming-in side streams (S_{Vi} and S_{Li}) above the feed plate.

Our complete dynamic model consists of:

$$\frac{d(M_1 + M_w)}{dt} = \hat{V}_2 - \tilde{L}_1 - W - \tilde{V}_1 \tag{16}$$

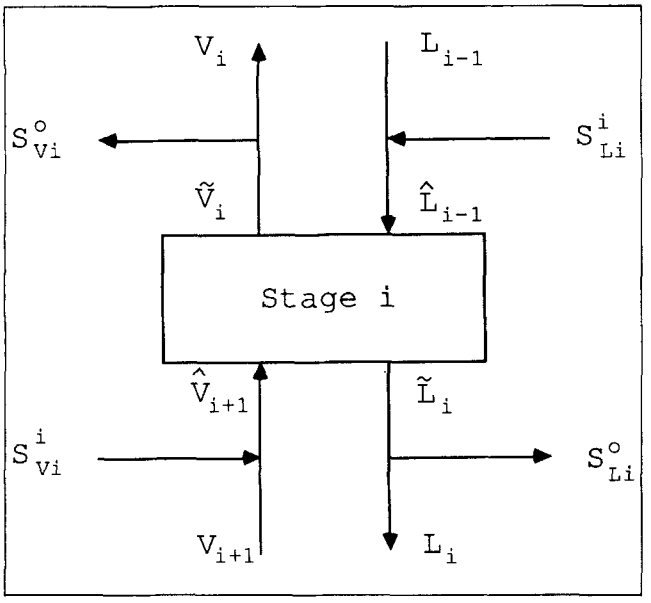

Figure 4. Flows around stage *i* of a crude tower.

Table 1. Degrees of Freedom Analysis for the Crude Tower

Unknown Variables		
Type	Variables	No.
Holdup	M_i, M_w	N+1
Flow Rates	L_i, V_i	2N
	D, W, S_1-S_4, S_p	7
Temperature	T_i	N
Heat Input	Q_c, Q_r, Q_p	3
Composition	$x_{i,j}$	NC-1
Equations		
Type	Eq. No.	No.
Composition	17-18, 21	NC
Enthalpy	19, 22	N
Equilibrium	23-25	NC
Summation	26-28	2N
Weir	29	N-6
Degrees of Freedom		
No. of Unknowns	2NC+4N+10	
No. of Equations	2NC+4N-6	
Degrees of Freedom	16	

$$\frac{d(M_1x_{1,j})}{dt}=\hat{V}_2\hat{y}_{2,j}-\tilde{L}_1x_{1,j}-\hat{V}_1y_{1,j}\quad j=1,\ldots,C-1 \tag{17}$$

$$\frac{dM_w}{dt}=\hat{V}_2\hat{y}_{2,C}-W-\tilde{V}_1y_{1,C} \tag{18}$$

$$\frac{d(M_1h_1+M_wh_w)}{dt}=\hat{V}_2\hat{H}_2-\tilde{L}_1h_1-Wh_w-\tilde{V}_1H_1+Q_c \tag{19}$$

$$\frac{dM_i}{dt}=\hat{L}_{i-1}+\hat{V}_{i+1}-\tilde{L}_i-\hat{V}_i\quad i=2,\ldots,N \tag{20}$$

$$\frac{d(M_ix_{i,j})}{dt}=\hat{L}_{i-1}\hat{x}_{i-1,j}+\hat{V}_{i+1}\hat{y}_{i+1,j}-\tilde{L}_ix_{i,j}-\tilde{V}_iy_{i,j},$$
$$i=2,\ldots,N;\ j=1,\ldots,C \tag{21}$$

$$\frac{d(M_ih_i)}{dt}=\hat{L}_{i-1}\hat{h}_{i-1}+\hat{V}_{i+1}\hat{H}_{i+1}-\tilde{L}_ih_i-\tilde{V}_iH_i+Q_i,$$
$$i=2,\ldots,N \tag{22}$$

$$y_{1,j}=K_{1,j}x_{1,j}\quad j=1,\ldots,C-1 \tag{23}$$

$$y_{1,C}=P_w/P_1 \tag{24}$$

$$y_{1,j}=K_{i,j}x_{i,j}\quad i=2,\ldots,N;\quad j=1,\ldots,C \tag{25}$$

$$\sum_{j=1}^{C-1}x_{1,j}=1 \tag{26}$$

$$\sum_{j=1}^{C}x_{i,j}=1\quad i=2,\ldots,N \tag{27}$$

$$\sum_{j=1}^{C}y_{i,j}=1\quad i=1,\ldots,N \tag{28}$$

$$M_i=f_w(\tilde{L}_i)\quad \text{for all } i\neq 1, 28, 31, 33, 35, 37 \tag{29}$$

Degree of freedom analysis and control configuration

A degree of freedom analysis should be the first step in the development of a dynamic simulator as well as the design of a control system, especially for a complex system like a crude tower. With the feed conditions and the column pressures specified, the dynamic model of the crude tower was found to have 16 degrees of freedom, as summarized in Table 1. This implies that one can control up to 16 variables. Although it is not necessary to implement all 16 control loops in practice, one still has to identify and provide the same number of relationships among process variables in the form of either control laws or variable specifications before attempting to develop a dynamic simulator. Hence, at this point it will be a logical step to discuss our control configuration for the tower. Table 2 summarizes how the 16 degrees of freedom were specified in this work. First, end points (EP) of the five major products—gasoline (EP_1), naphtha (EP_2), kerosene (EP_3), light gas oil (LGO) (EP_4), heavy gas oil (HGO) (EP_5)—were controlled by manipulating their product rates. 90% true-boiling-point (TBP) distillation point was chosen as the end point characterizing each product quality. The TBP points were evaluated following the procedure in the literature (Rice, 1988). Next, seven SISO PI control loops were used to regulate the holdups of the accumulator and the bottom in the main column, and the holdups of the reboiler and the bottoms in the side strippers. The holdups in the main column were controlled by manipulating the leaving liquid streams, while those in the side strippers were controlled by the side draw rates from the main column.

Finally, the remaining four degrees of freedom were specified by holding the four variables shown in Table 2 constant

Table 2. Specification of 16 Degrees of Freedom for the Crude Tower

Class	Controlled Variables	Manipulated Variables
Product Quality Control	EP_1	D
	EP_2	L_{31}
	EP_3	L_{33}
	EP_4	L_{35}
	EP_5	L_{37}
Level Control	M_1	L_1
	M_w	W
	M_{28}	L_{28}
	M_{31}	S_1
	M_{33}	S_2
	M_{35}	S_3
	M_{37}	S_4
Fixed Variables	V_1/L_1	S_p
	V_{31}/L_{31}	Q_p

at their base operating levels. The purpose of the pumparound (S_p and Q_p) is to maximize product yields and energy recovery. Pumparound control was not included in our work because an optimal operation is usually obtained at the maximum rate within process limits and its control is thus separated from product quality control structure (Muske, 1991a). Two fixed vapor/liquid ratios in Table 2 imply that the heat duties of the condenser and the reboiler (Q_c and Q_r) were assumed to be perfectly adjusted to maintain the specified ratio levels.

Dynamic stagewise adiabatic flash algorithm

The algorithm proposed earlier for a single flash stage (ISS model) was extended for solving the dynamic model of the crude tower. The basic idea underlying the extension is to regard a multistage column as a stack of flash stages and then perform dynamic adiabatic flash calculation for each stage in a sequential manner. In other words, an implicit numerical algorithm (the ISS model) is applied to each stage separately while the inputs to each stage, which come from surrounding stages, are assumed to be constant for the implicit integration time step (0.002 h). That is, after each 0.002 h of simulation, the flow rates, compositions, and enthalpy of the feed streams to each stage are updated. Therefore, the dynamic stagewise adiabatic flash (DSAF) algorithm is implicit for each stage for a short simulation time period, but is applied explicitly for the entire column. Specifically, for stage i at time step $t^{(n)}$, a pseudo-feed stream is set up as:

$$F^{(n+1)} = \hat{L}_{i-1}^{(n+1)} + \hat{V}_{i+1}^{(n)} \tag{30}$$

$$z_j^{(n+1)} = \frac{\hat{L}_{i-1}^{(n+1)}\hat{x}_{i-1,j}^{(n+1)} + \hat{V}_{i+1}^{(n)}\hat{y}_{i+1,j}^{(n)}}{F^{(n+1)}}, \quad j = 1, \ldots, C \tag{31}$$

$$h_F^{(n+1)} = \frac{\hat{L}_{i-1}^{(n+1)}\hat{h}_{i-1}^{(n+1)} + \hat{V}_{i+1}^{(n)}\hat{H}_{i+1}^{(n)}}{F^{(n+1)}} \tag{32}$$

Then the single flash stage calculation updates the dynamic state of stage i, and the effluent streams serve as a feed stream for the adjacent stages.

Typically V_i and T_i were chosen as independent variables to drive to zero the mismatches in mass and energy balances expressed in a form similar to Eq. 12. Heat duties Q_c and Q_r were substituted for vapor flow rates for the condenser-accumulator and the reboiler, respectively, because the vapor/liquid ratios were specified as the degrees of freedom. Two immiscible liquid phases on the accumulator necessitated the use of another independent variable. The balance equations for stage 1 were recast in terms of a total holdup $M_{1t}(=M_1+M_w)$ and a water phase fraction $\phi_w(=M_1/M_{1t})$. Then a three-element independent vector was solved with an additional mass balance mismatch function:

$$\theta = (\phi_w, Q_c, T_1)^T \tag{33}$$

$$f_1(\theta) = \frac{y_{1,C}}{P_w/P_1} - 1 \tag{34}$$

Stagewise calculations may proceed either from top to bottom or from bottom to top. Since a pseudo-feed for each stage is only set up explicitly as shown in Eqs. 30-32, any change introduced at one end of the column will not be accounted for during the stage calculation at the other end until a sufficient number of integration steps are carried out. In other words, an artificial dead time may be induced by the algorithm. To reduce this effect, an alternating direction scheme was used. Specifically, for a given time step Δt, stagewise calculation was carried out from top to bottom for the first half step, followed by calculation in the reverse order for the next half.

The DSAF algorithm efficiently provided stable solutions for an extensive range of system upsets. A two-hour transient response for a 10% feed enthalpy change could be obtained in ~4 min on a 50 MHz 486 PC (approximately 1.5 Mega Flops) using a Microsoft 5.1 FORTRAN complier with $\Delta t = 0.002$ h, which is more than 20 times faster than real time. It should be noted that a fully implicit integration of the entire column (a dynamic version of the 2N Newton-Raphson method, Holland, 1981) was implemented and found to require more than 60 times as much CPU as the DSAF algorithm and found to exhibit occasional convergence problems.

Open-loop responses

Two open-loop responses are presented in this section to discuss the major dynamic characteristics of the crude tower in relation to its product quality control. For the open-loop responses, the regulating controls (that is, level controller) were left in service while the product quality control loops were made inoperative. The base conditions of the feed and the product streams are briefly outlined in Table 3. Detailed steady-state operating conditions of the tower can be found in the literature (Holland, 1981). A hydraulic time constant of 10 s was used to describe the liquid dynamics on each tray (Franks, 1972). Each holdup in the accumulator, the reboiler and the bottoms was assumed to initially have a 10 min residence time based on the leaving liquid stream flow rate. All the levels were PI-controlled at 0.002 h intervals with relatively tightly tuned parameters, $K_c = 20\ h^{-1}$, $\tau_I = 0.3$ h. The DSAF algorithm used an integration time step, $\Delta t = 0.001$ h.

Figure 5 shows the open-loop responses of the product end points for a 4.54 kmol/h (8.2%) step increase in the kerosene product rate (L_{33}) introduced at $t = 0.1$ h. The end points of

Table 3. Base Conditions of Crude Feed and Product Streams

Crude Feed	Rate Enthalpy		998.3 kmol/h 55,400 kcal/kmol	
Product	End Point (K)		Rate (kmol/h)	
Gasoline	EP_1	373.2	D	73.1
Naphtha	EP_2	436.3	L_{31}	131.4
Kerosene	EP_3	472.8	L_{33}	55.4
LGO	EP_4	551.2	L_{35}	148.9
HGO	EP_5	644.1	L_{37}	48.6

Table 4. Open-Loop Process Gain Array

Output	Input (K·h/kmol)				
	D	L_{31}	L_{33}	L_{35}	L_{37}
EP_1	0.185	0.003	−0.0002	0.003	−0.002
EP_2	0.529	0.552	0.028	0.015	−0.004
EP_3	0.553	0.665	0.513	0.030	−0.004
EP_4	0.590	0.718	0.710	0.634	0.009
EP_5	1.568	1.870	1.851	1.870	1.258

kerosene and heavier products increased significantly, while lighter products showed negligible changes. This illustrates the well-known *one-way interaction* characteristics of the product quality control loops in a crude tower (McAvoy, 1983). This behavior also manifests itself in an open-loop process gain array shown in Table 4, which was obtained by increasing each product rate by 4.54 kmol/h separately. The array has a triangular form in the sense that the upper-diagonal elements have negligible magnitudes in comparison with the diagonal and subdiagonal elements. The mechanism of the one-way interaction can be explained as follows. An increase in a side product rate will lower its holdup level, triggering a compensating action by the level controller to increase a side draw from the main column. Accordingly the liquid traffic in the main column will be reduced below the draw tray, but this upset will not propagate upward significantly.

Figure 6 shows product quality responses for a change to a lighter crude feedstock. The lighter feed was simulated by increasing by 5% (relative) the mole fractions of component 1 through 24 which account for approximately half of the hydrocarbon fractions of the feed, and by decreasing the fractions of heavier components by the same magnitude. An inverse response was observed for each side product stream. More vapor was flashed from the lighter feed and rapidly propagated upward due to negligible vapor holdups on trays. This initially increased the internal vapor/liquid ratios, leading to a heavier liquid composition on each tray. But this trend started to be reversed as the reflux (L_1) was increased steadily by the accumulator level controller as the increased vapor rate raised the level in the accumulator. Figure 7 shows this transition as observed on tray No. 11, the draw tray for the second side stripper. Similar inverse responses were also observed for feed rate changes.

The crude column under study showed significant nonlinear behavior which is demonstrated by the variation of process gains when step changes in the input variables are reversed. The elements of the process gain array obtained by decreasing and increasing each product rate by 10% separately showed −10 to 120% increases in magnitude as compared to the process gains at the base case. A similar behavior was also observed for step changes in the feed rate and the feed enthalpy.

Nonlinear Model Based Product Quality Control

For all the crude column quality control studies performed, the dynamic model presented in the previous section was treated as the crude column. Two steady-state crude column models are used as part of the product quality controllers and should not be confused with the dynamic column model.

The primary control objective of a crude tower is to maintain the quality of product streams on specification. For the product quality control of the crude tower shown in Figure 1, the five controlled variables were chosen as the end points of five major product streams characterized by 90% TBP distillation points (see Table 2).

An RGA pairing analysis based on the linear transfer function models of the tower indicated that the product rate should be used to control its own end point (Hsie, 1989). Due to severe interaction among the loops, however, a multiple SISO-loop

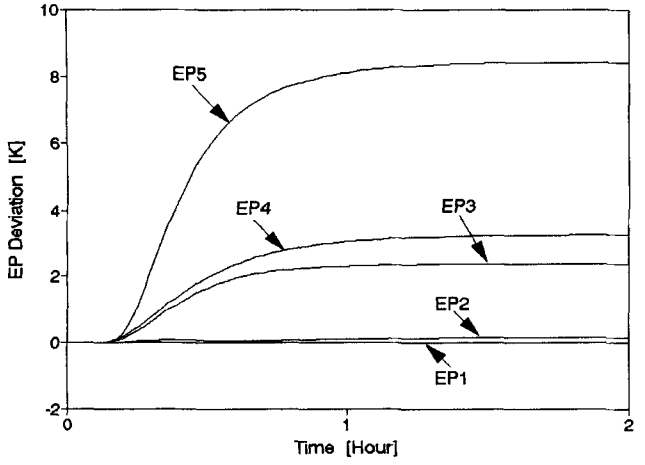

Figure 5. Open-loop end point responses to 4.54 kmol/h step increase in the kerosene product rate (L_{33}).

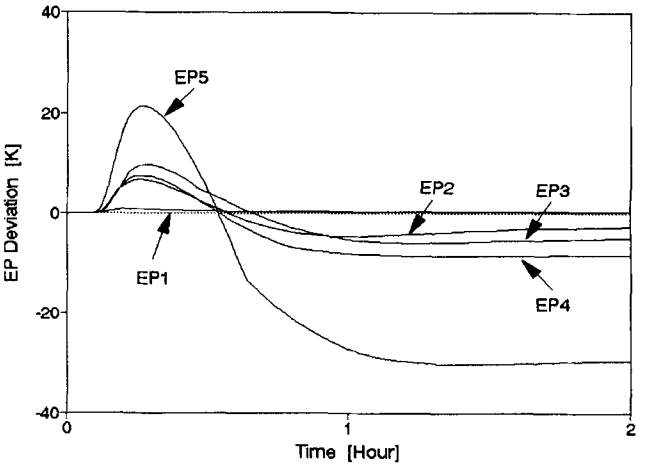

Figure 6. Open-loop end point deviations to a lighter feedstock change.

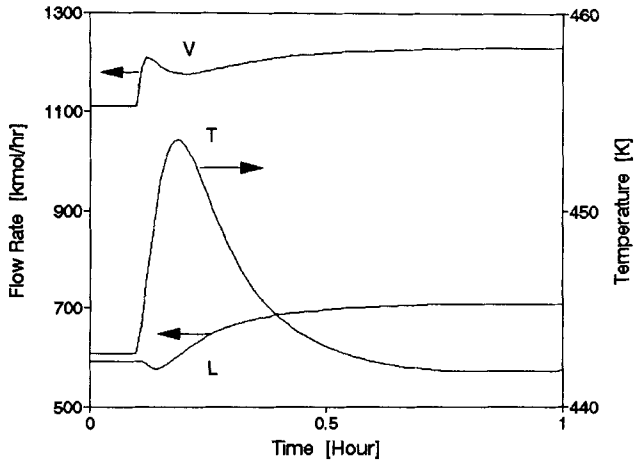

Figure 7. Open-loop responses of tray no. 11 to a lighter feedstock change.

configuration could not give a satisfactory performance without an effective decoupler (Hsie, 1989). In this work, to overcome the interaction of the loops, nonlinear PMBC schemes comprising GMC control laws and approximate steady-state models are employed. Two steady-state models are described and compared for their control performance below.

Nonlinear PMBC models

Tray-to-tray Model. A rigorous steady-state model of the tower can be obtained from the dynamic model (Eqs. 16–29) simply by setting the derivative terms to 0 and omitting the weir formula. The resulting model has 9 degrees of freedom since holdup variables do not appear in the model.

A steady-state version of the DSAF algorithm is used iteratively to find a convergent solution until the relative change in stage temperatures between two iterations becomes sufficiently small, that is

$$\max \left| \frac{T_i^{(k+1)} - T_i^{(k)}}{T_i^{(k)}} \right| \leq 10^{-5} \tag{35}$$

The stage temperatures were found to be the most sensitive variable and, therefore, were selected as the convergence criteria. The number of iterations required varied depending on the size of the upset, and typically ranged from 100 to 200 iterations with 20–40 CPU s on a 50 MHz 486 PC.

To speed up the computation, a reduced component scheme was employed as follows. Since the typical composition profile shows a localized distribution of components depending on tray location, components whose pseudo-feed mole fractions were less than ϵ were excluded from the flash calculation on the corresponding stage. For $\epsilon = 10^{-6}$ about 25% reduction in CPU time could be realized without sacrificing accuracy. The EP predictions from the tray-to-tray model were in good agreement with the steady-state results from dynamic simulation within ~1% error.

Sectionwise Smith Brinkley (SSB) model. The Smith-Brinkley (SB) method is a shortcut design method for multistage separation processes (Smith and Brinkley, 1960a). When applied to a conventional distillation column under the assumptions of constant molar flow rates and K-values within each of rectifying and stripping section, SB model efficiently calculates the fraction of each component recovered in the bottom product as a solution of general difference equations (Smith and Brinkley, 1960b).

For columns with a complicated side stream structure as shown in Figure 1, however, it is not possible to divide the column into just a few sections without nullifying the constant molar flow assumptions and the difference equation solving procedure. One can at best expect to group several adjacent trays into a section in such a way that no side stream leaves or enters the section in the middle. For our model crude tower this sectioning procedure results in 18 sections, amounting to a reduction of the number of trays of about one half.

Another modification was necessary before performing the SB calculation on each section. Since the flow rate and the temperature profiles show such steep variations across the tower at normal operating conditions, the assumptions of constant molar flow and temperature are far from reality even in a section. To reduce the error arising from these implausible assumptions, both material and energy balances were enforced on each section to find "tuned" average flow rates and average temperature on which the SB calculation is based. This modified SB calculation for an n-trayed section shown in Figure 8 can be summarized as follows.

Given the conditions of the pseudo-feed streams L_0 and V_{n+1}, find V_1 and T_{avg} which satisfy:

(Total Mass)

$$\hat{L}_0 + \hat{V}_{n+1} = \tilde{L}_n + \tilde{V}_1 \tag{36}$$

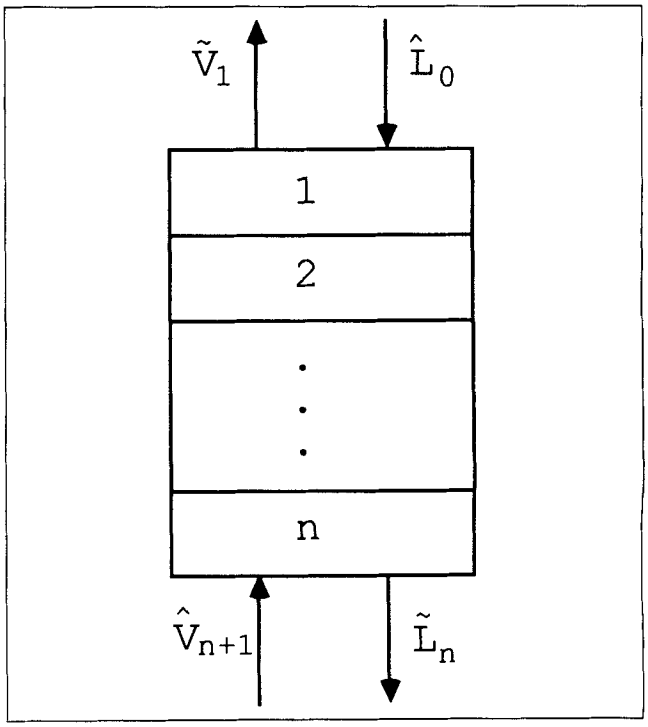

Figure 8. A typical *n*-trayed section for the SSB model.

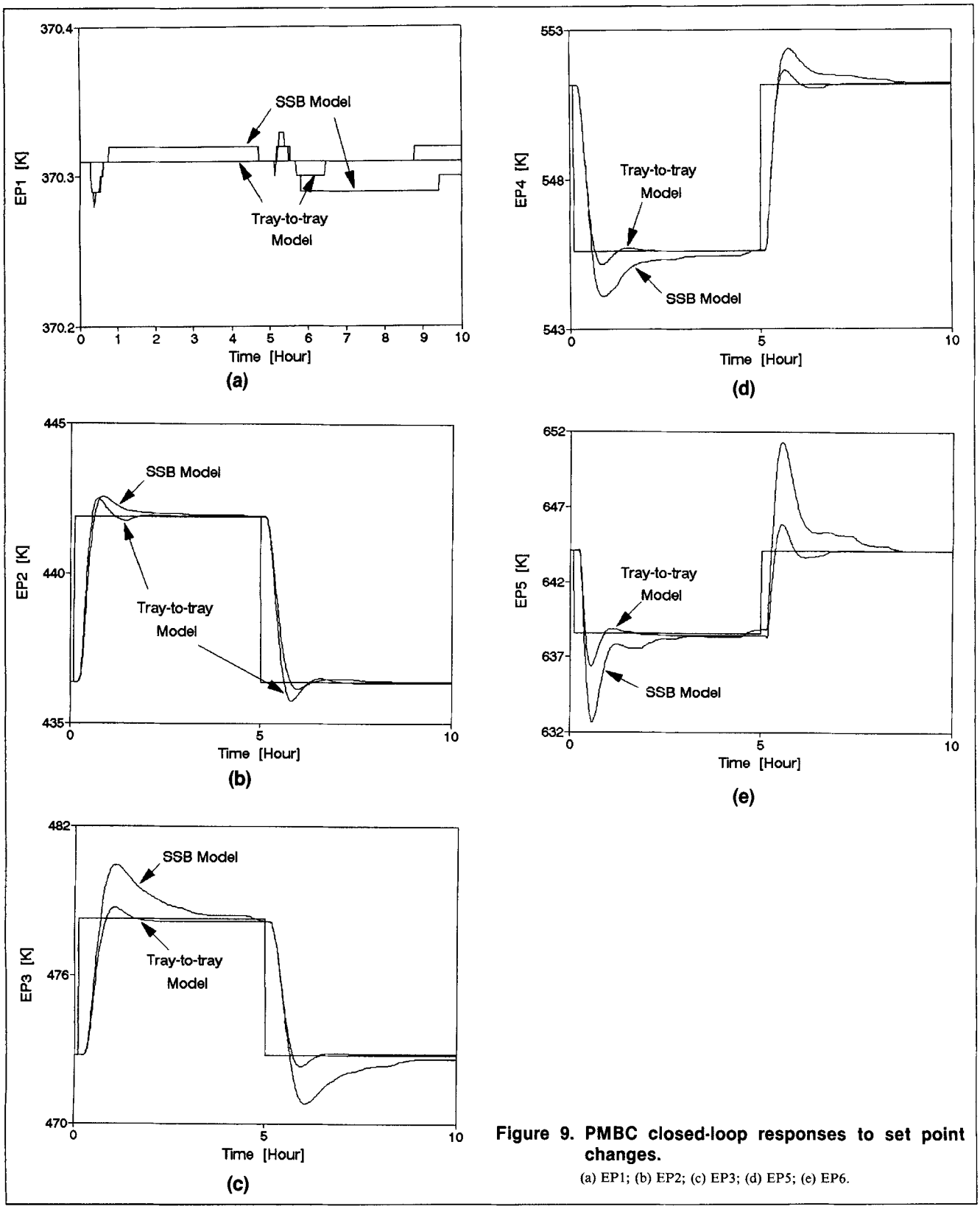

Figure 9. PMBC closed-loop responses to set point changes.

(a) EP1; (b) EP2; (c) EP3; (d) EP5; (e) EP6.

(Composition)

$$\hat{L}_0\hat{x}_{0,j}+\hat{V}_{n+1}\hat{y}_{n+1,j}=\tilde{L}_n x_{n,j}+\tilde{V}_1 y_{1,j},\quad j=1,\ \ldots,\ C \qquad (37)$$

(Enthalpy)

$$\hat{L}_0\hat{h}_0+\hat{V}_{n+1}\hat{H}_{n+1}=\tilde{L}_n h_n+\tilde{V}_1 H_1 \qquad (38)$$

Table 5. Steady-State End Point Deviations of the SSB Model

Case	ΔEP_1	ΔEP_2	ΔEP_3	ΔEP_4	ΔEP_5
Base	−3.289	−4.216	−1.952	−0.312	16.917
After Setpoint Changes (Figure 9)	−3.331	−2.374	−1.943	−0.634	19.699
After Feed Change (Figure 11)	−3.372	−4.711	−2.558	−0.703	16.531

(Separation)

$$\frac{\tilde{L}_n x_{n,j}}{\hat{L}_0 \hat{x}_{0,j} + \hat{V}_{n+1} \hat{y}_{n+1,j}} = \frac{(1 - S_j^n) + q_j (S_j^n - S_j)}{1 - S_j^{n+1}}, \quad j = 1, \ldots, C \tag{39}$$

$$S_j = \frac{K_j(T_{avg}) V_{avg}}{L_{avg}}, \quad j = 1, \ldots, C \tag{40}$$

$$q_j = \frac{\hat{L}_0 \hat{x}_{0,j}}{\hat{L}_0 \hat{x}_{0,j} + \hat{V}_{n+1} \hat{y}_{n+1,j}}, \quad j = 1, \ldots, C \tag{41}$$

$$L_{avg} = (\hat{L}_0 + \tilde{L}_n)/2 \tag{42}$$

$$V_{avg} = (\tilde{V}_1 + \hat{V}_{n+1})/2 \tag{43}$$

The effluent streams serve as a pseudo-feed stream for other sections, and a sequential sectionwise calculation is carried out in alternating directions as in the stagewise flash calculation for the dynamic tray-to-tray model. A reduced component scheme was also used to enhance computation speed. Convergence was obtained about twice as fast as the tray-to-tray steady-state model as a result of sectioning.

However, accurate steady-state prediction of the tower could not be obtained with the SSB model due to its inherent deficiencies. As shown in Table 5, predictions of the product end points were lower than the true values except for the heaviest product, which suggests that the calculated end point profile across the tower crosses the true one. Tests on a number of different operating conditions confirmed these observations.

This suggested a feasible model parametrization scheme for the SSB model which would improve its performance in a control application. End point prediction errors at a steady-state were treated as *biases* to shift the model calculations at each control step. Since the biases do not change a lot over the range of operation studied, these biases were chosen as our model parameters. The biases are updated at a new steady state on the basis of process measurements. Although it is common to choose the total number of stages as a model parameter in a distillation column control using a SB model (Ramchandran, 1992), such a scheme was found not to be feasible for a crude tower comprising 18 sections as a result of the complicated vapor and liquid profiles through a crude column.

Nonlinear PMBC strategy

A PMBC strategy using GMC control laws and steady-state models has been described in detail in a number of publications (Cott et al., 1989; Riggs and Rhinehart, 1990). A brief outline of the strategy will serve our purpose here. Assuming first-order dynamics between the output and its steady-state equivalent, GMC laws provide a steady-state target value for each product stream l:

$$EP_{l,ss} = EP_l + K_{l,1}(EP_{l,sp} - EP_l) + K_{l,2} \int_0^t (EP_{l,sp} - EP_l) dt \tag{44}$$

Then a steady-state model is solved iteratively to find a set of product rates which match the specified target values.

For each steady-state model, the Newton-Raphson method was used to simultaneously solve for the five product rates matching the target end points. The Jacobian was calculated using a finite difference scheme. An alternative method would be to take advantage of the one-way interaction characteristics of the loops and find each product rate one by one starting from the top. Both methods were tested in control studies and were found to show comparable performances in CPU time and accuracy.

Control performances

The two nonlinear PMBC models were compared for their set point tracking and disturbance rejection capabilities. Six-minute analyzer delays was assumed for each of the five products in the control simulations. Only proportional action was used for GMC controllerse with the tray-to-tray model, and was tuned at $K_1 = 1.25$ for all the loops using an ISE criterion for set point changes. On the other hand integral actions were necessary with the SSB model to remove the offset caused by its prediction error. The ISE criterion was used again for tuning of $K_2 = 0.7\ h^{-1}$ for all the loops.

Figures 9a-9e show the set point tracking performances of the two nonlinear PMBC controllers. The set point for EP_1 remained unchanged; the set points for EP_2 and EP_3 were increased by 5.56 K at $t = 0.1$ h, and reset to the base condition at $t = 5$ h; those for EP_4 and EP_5 were changed in the reverse fashion. The tray-to-tray model showed good performance for all the product streams; this demonstrates its inherent nonlinear decoupling capability in the presence of strong interactions among the loops. As a result of the close match with the dynamic simulator for steady-state predictions, any significant

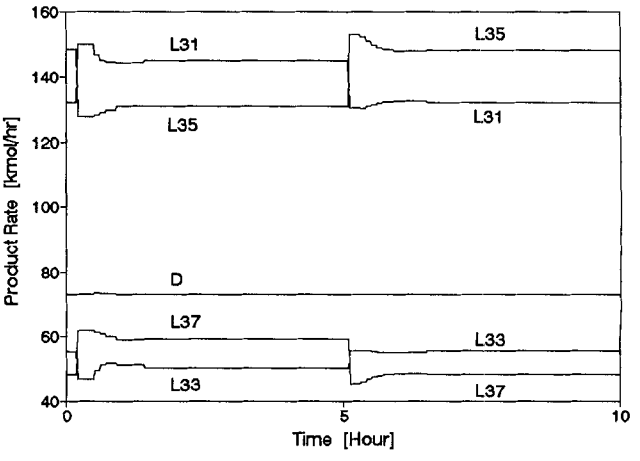

Figure 10. Product rates from the tray-to-tray model during set point changes.

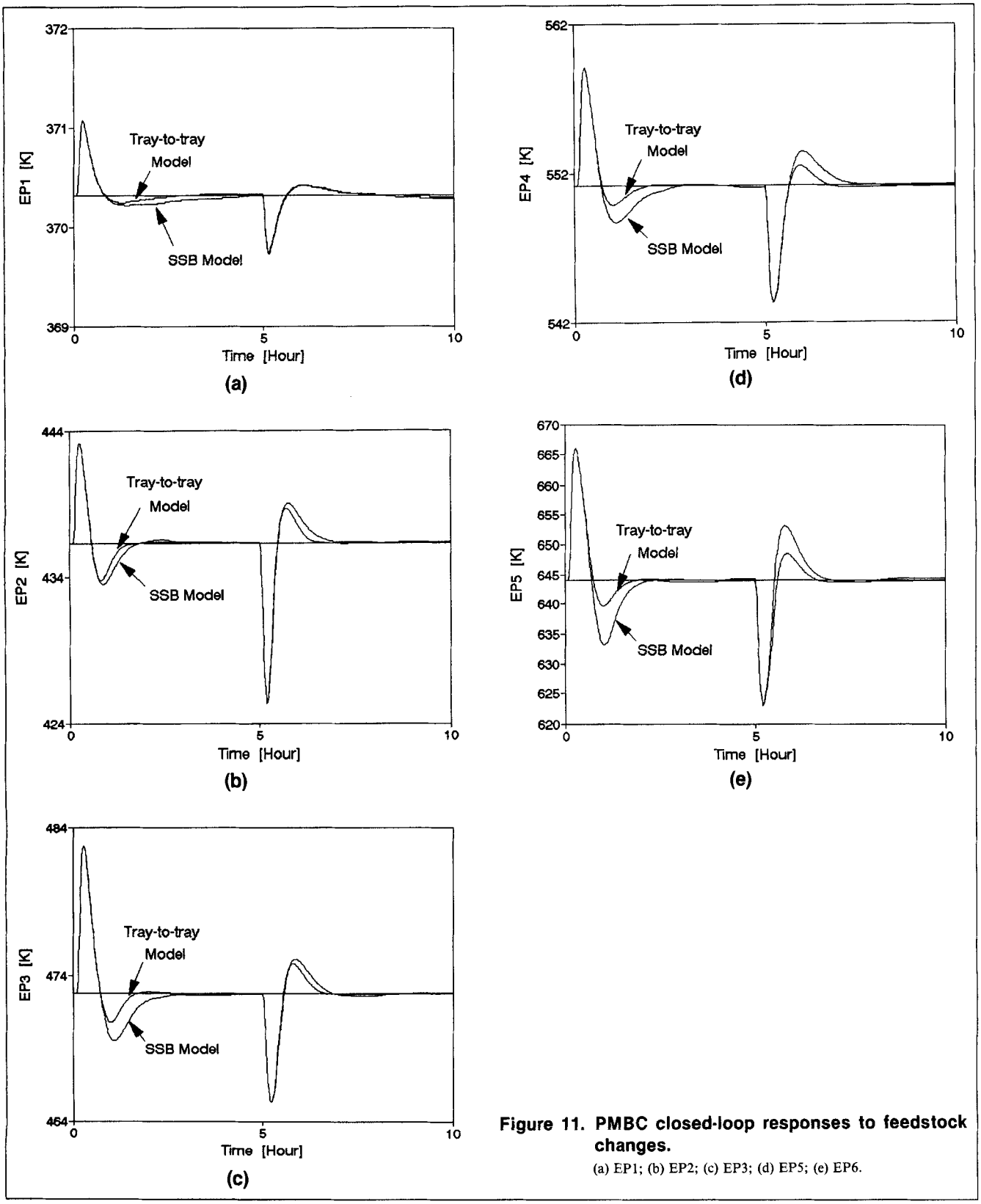

Figure 11. PMBC closed-loop responses to feedstock changes.

(a) EP1; (b) EP2; (c) EP3; (d) EP5; (e) EP6.

offsets were not observed even without integral action. Figure 10 shows the manipulated product rates calculated by the tray-to-tray model during this set point tracking.

The SSB model showed a somewhat degraded performance with larger overshoot and longer settling times due to its prediction error. Still the responses attest to a fairly good decoupling capability of an approximate model based control. Model prediction errors were evaluated at $t = 5$ h and were

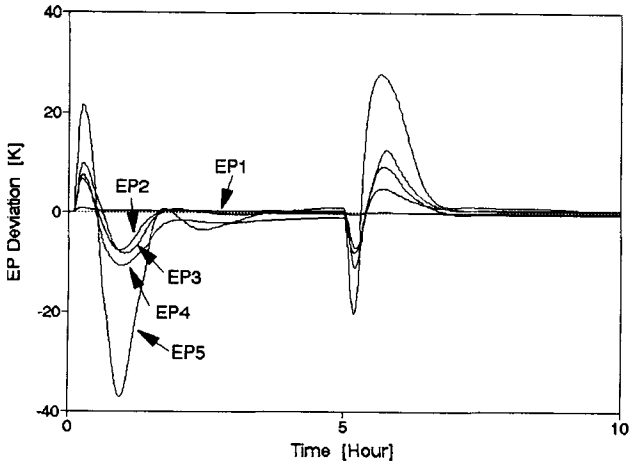

Figure 12. PI closed-loop responses to feedstock changes.

used as new biases for the next set point changes. Table 5 compares the biases calculated initially and at $t = 5$ h; a fair match between the two sets shows the feasibility of the bias adjustment scheme for model parametrization purposes of the SSB model.

Figures 11a–11e show closed-loop responses to crude feed stock changes. A lighter feed (in the sense explained earlier) was introduced at $t = 0.1$ h, and was switched back to the original at $t = 5$ h. Overall good disturbance rejection was obtained except for the initial big peaks following each feed change. These peaks are similar to the open-loop peaks in Figure 6, and mainly resulted from the analyzer delay: the feed disturbances were passed to the tower without facing any compensating action during the initial 6 min control interval. But a closer examination of the peaks in Figure 6 and Figures 11a–11e revealed that these closed-loop peaks are slightly higher than the open-loop peaks. This arose from the nonminimum phase behavior of the tower to feed stock changes which the steady-state model based controllers do not consider. The controllers increased the product rates during a few control intervals on the basis of their steady-state model predictions when the opposite action was desired.

It may be of interest to see how conventional PI controllers would perform for this highly interacting multivariable system. Figure 12 shows the end point deviations from the set points under the same feed stock switching scheme as in Figures 11a–11e. Multiple SISO PI controllers were tuned for this disturbances by a time-consuming trial and error procedure. Responses comparable to the PMBC results were obtained except for larger overshoots.

However, unacceptable responses were obtained for the set point changes as in Figures 9a–9e with the same controller parameters: the responses of light products were too sluggish while those of heavy products moved initially in the opposite direction to the set point changes. In fact, we could not find PI parameters which would yield fair performance both for set point tracking and disturbance rejection from our extensive, if not exhaustive, trial and error tuning. As mentioned earlier, it is not surprising to find that simple SISO-loop PI controllers failed to handle a highly interacting system like a crude tower without employing an additional advanced scheme like a decoupler.

Conclusions

A novel dynamic simulation algorithm was developed for a crude tower. The algorithm proceeded sequentially with a dynamic adiabatic flash calculation on each stage, where both temperature and vapor flow rate were solved simultaneously based on both the mass and energy balances. The algorithm called DSAF provided stable and accurate solutions more than 20 times faster than real time, while the conventional bubble-point algorithm showed inherent instability in the face of enthalpy inversion stemming from the extremely wide-boiling nature of the crude feed.

Two nonlinear PMBC schemes based on GMC control laws and steady-state models were investigated for the product quality control of a simulated crude tower. A nonlinear PMBC scheme using a rigorous tray-to-tray model showed a good performance both for set point changes and for feed composition changes. Another scheme using an approximate sectionwise Smith-Brinkley model showed a slightly poorer performance, but yet demonstrated its capability of decoupling the strong interaction among the loops. The disturbance rejection performances of both nonlinear PMBC controllers were limited by the inverse action between the feed disturbances and the controlled variables for the crude column studied.

Notation

C = number of components
D = overhead product rate, kmol/h
E = total energy holdup on a tray, kcal
EP_l = end point of the lth product stream, K
F = feed flow rate, kmol/h
h = molar liquid enthalpy, kcal/kmol
h_F = molar feed enthalpy, kcal/h
h_j = pure-component liquid enthalpy of component j, kcal/kmol
H = molar vapor enthalpy, kcal/kmol
H_j = pure-component vapor enthalpy of component j, kcal/kmol
$K_{l,1}$ = GMC proportional gain for the lth loop
$K_{l,2}$ = GMC integral parameter for the lth loop, 1/h
K_c = proportional gain of PI level controller, 1/h
K_j = K value of component j
$K_{i,j}$ = K value of component j on stage i
L = liquid flow rate, kmol/h
M = holdup, kmol
M_i = holdup on stage i, kmol
N = number of stages
P = pressure, Pa
P_w = water vapor pressure, Pa
q_j = liquid feed fraction of jth component for SB section
Q_p = pump-around heat duty, kcal/h
S = stripping factor, Eq. 37
S_i = side draw rate for ith side stripper, kmol/h
S_{Li} = liquid side stream rate around stage i, kmol/h
S_{Vi} = vapor side stream rate around stage i, kmol/h
T = temperature, K
T_i = temperature on stage i, K
V = vapor flow rate, kmol/h
V_i = flow rate of vapor leaving stage i, kmol/h
W = water flow rate from accumulator, kmol/h
$x_{i,j}$ = liquid mole fraction of component j on stage i
x_j = liquid mole fraction of component j
$y_{i,j}$ = vapor mole fraction of component j on stage i
y_j = vapor mole fraction of component j
z_j = feed mole fraction of component j

Greek letters

Δt = integration time step size, h
ϵ = tolerance for reduced-component scheme

θ = independent vector in dynamic adiabatic flash calculation
τ_1 = integral time of PI level controller, h
ϕ_w = fraction of water phase in the accumulator

Subscripts

avg = average
C = water (the last numbered component in the crude feed)
F = feed
i = stage number
j = component number
sp = set point
t = total
w = water
w = weir, Eqs. 7 and 26

Superscripts

i = coming-in side stream
(k) = iteration counter for stagewise calculation, Eq. 32
(n) = integration time step counter
^{o} = going-out side stream
$'$ = pseudo-feed condition

Literature Cited

Adams, G. F., "Computer Controls Crude Unit," *Hydroc. Proc. & Petrol. Refiner*, **41**(5), 137 (May, 1962).

Ballard, O., and C. Brosilow, "Dynamic Simulation of Multi-Component Distillation Columns," AIChE Meeting, Miami (1978).

Bequette, B. W., "Nonlinear Control of Chemical Processes: A Review," *Ind. Eng. Chem. Res.*, **30**, 1391 (1991).

Cecchetti, R., J. L. Niedzwiecki, and D. Holland, "Pipestill Products Verify these Computer Estimates," *Hydroc. Proc.*, **42**(9), 159 (Sept., 1963).

Cott, B. J., G. Durham, P. L. Lee, and G. R. Sullivan, "Process Model-Based Engineering," *Comput. Chem. Eng.*, **13**, 973 (1989).

Cutler, C. R., and B. L. Ramaker, "Dynamic Matrix Control—A Computer Control Algorithm," AIChE Meeting, Houston (1979).

Economou, C. G., M. Morari, and B. O. Palsson, "Internal Model Control: 5. Extension to Nonlinear Systems," *Ind. Eng. Chem. Process Des. Dev.*, **25**, 403 (1986).

Franks, R. G. E., *Modelling and Simulation in Chemical Engineering*, Wiley, New York (1972).

Friday, J. R., and B. D. Smith, "An Analysis of the Equilibrium Stage Separations Problem—Formulation and Convergence," *AIChE J.*, **10**, 698 (1964).

Friedman, Y. Z., "Control of Crude Fractionator Product Qualities During Feedstock Changes by Use of a Simplified Heat Balance," paper TA-5:40, ACC Meeting, Boston (1985).

Gani, R., C. A. Ruiz, and I. T. Cameron, "A Generalized Model for Distillation Columns: I. Model Description and Applications," *Comput. Chem. Eng.*, **10**, 181 (1986).

Hess, F. H., PhD Diss., Texas A&M Univ., College Station (1977).

Hess, F. E., C. D. Holland, R. McDaniel, and N. J. Tetlow, "Solve More Distillation Problems: 7. Absorber-Type Pipestills," *Hydroc. Proc.*, **56**(5), 241 (May, 1977).

Holland, C. D., *Fundamentals of Multicomponent Distillation*, McGraw-Hill, New York (1981).

Hsie, W.-H. L., "Modeling, Simulation and Control of Crude Towers," PhD Diss., Univ. of Maryland, College Park (1989).

Lee, P. L., and G. R. Sullivan, "Generic Model Control (GMC)," *Comput. Chem. Eng.*, **12**, 573 (1988).

McAvoy, T. J., *Interaction Analysis*, Instrument Soc. of Am., Research Triangle Park, NC (1983).

Muske, K., J. Young, P. Grosdidier, and S. Tani, "Crude Unit Product Quality Control," *Comput. Chem. Eng.*, **15**, 629 (1991a).

Muske, K. R., D. A. Logue, M. M. Keaton, and R. A. Hayward, "Gain Scheduled Model Predictive Control of a Crude Oil Distillation Unit," AIChE Meeting, Los Angeles (1991b).

Parrish, J. R., and C. B. Brosilow, "Nonlinear Inferential Control," *AIChE J.*, **34**, 633 (1988).

Ramchandran, B., J. B. Riggs, and H. R. Heichelheim, "Nonlinear Plant-Wide Control: Application to a Supercritical Fluid Extraction Process," *Ind. Eng. Chem. Res.*, **31**, 290 (1992).

Rice, V. L., "New Approach to Dynamic Distillation Simulation: Accurate Dynamic and Steady-State Predictions in Real Time," PhD Diss., Oklahoma State Univ., Stillwater (1988).

Richalet, J. A., A. Rault, J. L. Testud, and Papon, "Model Predictive Heuristic Control," *Automat.*, **14**, 413 (1978).

Riggs, J. B, and R. R. Rhinehart, "Comparison Between Two Nonlinear Process-Model Based Controllers," *Comput. Chem. Eng.*, **14**, 1075 (1990).

Smith, B. D., and W. K. Brinkley, "General Short-Cut Equation for Equilibrium Stage Processes," *AIChE J.*, **6**, 446 (1960a).

Smith, B. D., and W. K. Brinkley, "Supplement to the General Short-Cut Equation for Equilibrium Stage Processes," Document 6352; Amer. Document Inst., Photoduplication Service, Library of Congress, Washington, DC (1960b).

Van Horn, L. D., and P. R. Latour, "Computer Control of a Crude Still," *Instrum. Tech.*, 33 (Nov., 1976).

Veland, L. H., J. Hoyland, C. R. Aronson, and D. C. White, "Unique Features Improved Crude Unit Advanced Control," *Hydrocarb. Proc.*, 73 (Sept., 1987).

Wade, H. L., C. J. Ryskamp, and R. B. Bryton, "Seven Ways to Up Crude-Unit Productivity," *Oil and Gas J.*, **75**, 83 (Feb., 1977).

Manuscript received Dec. 28, 1992, and revision received Jan. 20, 1994.